ELSEVIER

Journal of Alloys and Compounds 462 (2008) 201–208

Journal of ALLOYS AND COMPOUNDS

www.elsevier.com/locate/jallcom

Mechano-chemical activation synthesis (MCAS) of disordered $Mg(BH_4)_2$ using $NaBH_4$

R.A. Varin [a,*], Ch. Chiu [a], Z.S. Wronski [a,b]

[a] *Department of Mechanical Engineering, University of Waterloo, Waterloo, Ontario, Canada N2L 3G1*
[b] *CANMET Energy Technology Centre, Hydrogen Fuel Cells and Transportation, Natural Resources Canada, 1 Haanel Dr., Ottawa, Ontario, Canada K1A 1M1*

Received 17 July 2007; received in revised form 26 July 2007; accepted 27 July 2007
Available online 6 August 2007

Abstract

Mechano-chemical activation synthesis (MCAS) of a powder mixture ratio $2NaBH_4$ and $MgCl_2$ was carried out by ball milling in a magneto-mill from 1 to 100 h duration with the objective of initiating a metathesis reaction $2NaBH_4 + MgCl_2 \rightarrow Mg(BH_4)_2 + 2NaCl$. It is found from X-ray diffraction (XRD) that the reaction has been only partially completed resulting in the formation of NaCl and a $(Na,Mg)BH_4$ solid solution. The solutionizing effect of Mg becomes more intense as milling time increases. No XRD peaks of crystalline $Mg(BH_4)_2$ are observed. Although the result of XRD analysis in the present work does not indicate the presence of a crystalline $Mg(BH_4)_2$ hydride, the similarity of thermal events in the DSC test of the milled powder mixtures to those of crystalline $Mg(BH_4)_2$ [D.S. Stasinevich, G.A. Egorenko, Russ. J. Inorg. Chem. 13 (1968) 341–343; V.N. Konoplev, V.M. Bakulina, Izv. Akad. Nauk SSSR 1 (1971) 159–161] indicates the possibility of presence of a "disordered" $Mg(BH_4)_2$ in the in the milled powder mixture, as specifically proposed by Nakamori et al. [Y. Nakamori, K. Miwa, A. Ninomiya, H. Li, N. Ohba, S.-I. Towata, A. Züttel, S.-I. Orimo, Phys. Rev. B74 (2006) 045126; Y. Nakamori, H.-W. Li, K. Kikuchi, M. Aoki, K. Miwa, S. Towata, S. Orimo, J. Alloys Compd., in press, doi:10.1016/j.jallcom.2007.03.144]. It is hypothesized that the presence of $(Na,Mg)BH_4$ solid solution in the MCAS process inhibits the formation of crystalline $Mg(BH_4)_2$. Regardless of the nature of the synthesized hydride phase the milled powders desorb hydrogen within the 275–420 °C temperature range and the total amount of hydrogen desorbed gradually decreases with increasing milling time reaching ∼2.1 wt.% for the powder milled for 100 h. However, regardless of the milling time the total amount of hydrogen desorbed within 275–420 °C is always less than the theoretical hydrogen capacity in the initial mixture of $2NaBH_4$ and $MgCl_2$ (∼4.7 wt.%).

Keywords: Hydrogen storage materials; Magnesium borohydride; Sodium borohydride; Mechano-chemical activation synthesis; X-ray diffraction; Differential scanning calorimetry

1. Introduction

Complex hydrides based on light metals such as Mg, B, Li and Al are very attractive materials for solid state hydrogen storage since they possess very high volumetric and especially gravimetric hydrogen densities which can meet the 9 wt.% target by year 2015 [1–3] with flying colors. For example, a complex hydride based on the Mg–B–H system with the stoichiometric composition $Mg(BH_4)_2$ (magnesium borohydride or tetrahydroborate) has a theoretical gravimetric hydrogen density of ∼15 wt.% [1] which makes it very attractive as a solid-state hydrogen storage material. It is based on very inexpensive elements such as magnesium (Mg) and boron (B). It was synthesized by Russian researchers over 30 years ago by the exchange reaction (also called a "metathesis reaction") of sodium borohydride ($NaBH_4$) with anhydrous magnesium chloride ($MgCl_2$) in diethyl ether [4,5]. Its thermal decomposition was investigated [4,5] and several major endothermic effects related to hydrogen desorption have been found. However, the range of hydrogen desorption temperatures found is still far too high for fueling a proton exchange membrane (PEM) fuel cell, specifically, in automotive applications [1–3] although it might be suitable for fuel cells which allow higher working temperature such as solid oxide fuel cells (SOFCs). It is also to be pointed out that there is some experimental evidence of reversibility of $Mg(BH_4)_2$ by its direct synthesis from the elements reported in a 50-year-old German

* Corresponding author. Fax: +1 519 888 6197.
E-mail address: ravarin@mecheng1.uwaterloo.ca (R.A. Varin).

0925-8388/$ – see front matter © 2007 Elsevier B.V. All rights reserved.
doi:10.1016/j.jallcom.2007.07.110

patent by Goerrig [13]. The synthesis temperature and pressure were quite high and the yield of magnesium borohydride was not too large but the mere fact that the hydride could be synthesized from the elements is very encouraging.

Therefore, an important objective is to find the means which would substantially reduce the high temperatures of synthesis and decomposition of $Mg(BH_4)_2$ in order to make them more compatible with the requirements of the automotive PEM fuel cell [1–3]. In the past 10 years it has been recognized that the formation of *nanostructured* hydrides may improve their hydrogen storage properties [6–10]. The most effective method of simultaneous synthesis and nanostructuring of various hydrides is reactive mechanical milling/alloying [7]. Following this path, more recently, we attempted a direct mechano-chemical synthesis of $Mg(BH_4)_2$ by controlled reactive mechanical alloying (CRMA) of Mg and amorphous boron under 880 kPa pressure of hydrogen in a unique magneto-ball mill [11,12]. Completely different response of the synthesized Mg–2B mixture was observed depending on the chemical state of amorphous boron used for the synthesis. However, no evidence of the presence of crystalline $Mg(BH_4)_2$ has been observed using X-ray diffraction (XRD) [11,12].

A method of the synthesis of nanostructured complex hydrides which can be an alternative to the ball milling of elemental powders is mechano-chemical activation synthesis (MCAS) which occurs by high energy ball milling of a complex hydride (e.g. $NaAlH_4$) mixed with an appropriate metal di-or tri-chloride, MCl_n. In its essence this is a "metathesis reaction" in solid state instead of the one which uses diethyl ether as a solvent. This method has been extensively used for the synthesis of complex magnesium alanate hydrides by Dymova et al. [14,15], Mamatha et al. [16,17] and Kim et al. [18]. Jeon and Cho [19] and Srinivasan et al. [20] used MCAS for the synthesis of $Zn(BH_4)_2$. Very recently, Nakamori et al. [21,22] used MCAS for the synthesis of various metal borohydrides $M(BH_4)_n$ (M = Al, Ca, Cr Mg, Mn, Sc, Zr, Ti, V, Zn; n = 2–4). They used the mixture of metal chloride MCl_n and both $LiBH_4$ and $NaBH_4$ which were milled under argon (0.1 MPa) for 5 h. The reaction during milling was proposed to be as follows:

$$MCl_n + nLiBH_4 \rightarrow M(BH_4)_n + nLiCl \quad (M = Cr, Mg, Mn, Zr, Ti, V, Zn) \tag{1}$$

$$MCl_n + nNaBH_4 \rightarrow M(BH_4)_n + nNaCl \quad (M = Ca, Sc, Al) \tag{2}$$

X-ray diffraction (XRD) showed no peaks of starting materials of MCl_n and $LiBH_4$ after milling for 5 h when $LiBH_4$ was used as a reacting agent and all of the XRD peaks belonged to LiCl. However, when $NaBH_4$ was used with MCl_n where M = Ca, Sc and Al the diffraction peaks of $NaBH_4$ were still present in the diffraction patterns. When $NaBH_4$ was used with MCl_n where M = Cr, Mn, Ti, V, Zn then only the NaCl peaks shifted to lower diffraction angles were present. The authors concluded that the reaction of Eq. (1) when $LiBH_4$ was used is much easier than that of Eq. (2) with $NaBH_4$ due to similar ionic radii of Li^+ (0.076 nm) and M^+ in the solid-solid cation exchange reaction than that of Na^+ (0.102 nm). The most confusing result of their work is the absence of the XRD peaks of crystalline $M(BH_4)_n$ after milling regardless of whether $LiBH_4$ or $NaBH_4$ is used. According to Nakamori et al. this is due to the "disordering" of crystal structure of $M(BH_4)_n$. Instead, Nakamori et al. used Raman spectra to confirm the presence of $M(BH_4)_n$ after MCAS. However, Jeon and Cho [19] and Srinivasan et al. [20] observed very clearly XRD peaks of crystalline $Zn(BH_4)_2$ contrary to the results by Nakamori et al.

Neither Nakamori et al. [22] nor other researchers attempted to synthesize $Mg(BH_4)_2$ using $NaBH_4$. In the present work we report the results of the attempted MCAS synthesis of a nanostructured $Mg(BH_4)_2$ using $NaBH_4$ instead of $LiBH_4$. This is a continuation of our work on the direct synthesis of $Mg(BH_4)_2$ by reactive mechanical milling of elemental powders [11,12]. Although, as discussed above, Nakamori et al. concluded that MCAS reaction with $LiBH_4$ may be faster than that with $NaBH_4$, the former is a very expensive complex hydride (price ~$5700 per 1 kg of 95% purity $LiBH_4$ in the Alfa Aesar catalogue 2006–2007) and its application as a potential hydrogen storage material is very problematic. Moreover, as a result of MCAS synthesis according to the reaction in Eq. (1), $LiBH_4$ which has a very high theoretical hydrogen capacity of ~18.4% is converted through the reaction of Eq. (1) into another borohydride with a *lower* hydrogen capacity. Apparently, the usage of $LiBH_4$ in the synthesis of lower capacity borohydrides seems not to be very economical. On the top of it, $LiBH_4$ is a very volatile compound especially in contact with even traces of moisture.

For all the above reasons, we focused on $NaBH_4$ as a reacting compound in the reaction of Eq. (2) which was also used by Jeon and Cho [19] and Srinivasan et al. [20] for a successful synthesis of $Zn(BH_4)_2$. $NaBH_4$ is a very widely used compound in various sectors of industry, and its price is relatively low, about $280 per 1 kg of 98% pure compound (Alfa Aesar catalogue 2006–2007). It is much less volatile than $LiBH_4$. A controlled mechanical milling in a unique magneto-mill was employed for the MCAS synthesis.

2. Experimental

As received $NaBH_4$ (98% purity; Alfa-Aesar) and anhydrous $MgCl_2$ (99% purity; Alfa-Aesar) were mixed together in the 2:1 stoichiometric ratio (corresponding weight percents of $NaBH_4$ and $MgCl_2$ in the mixture are 44.3 and 55.7 wt.%, respectively, so as a result the weight ratio is ~1 g $NaBH_4$: 1.3 g $MgCl_2$). Subsequently, the mixture was subjected to controlled mechanical milling under 600 kPa pressure of high purity argon (99.999% purity) in the magneto-mill Uni-Ball-Mill 5 (A.O.C. Scientific Engineering Pty Ltd., Australia) [23–25]. Two Nd–Fe–B super-strong magnets at 6 and 8 o'clock positions which induce strong impact action of steel balls (milling mode designated as IMP68) with WD = 10 and 2 mm, respectively, were used where WD is the working distance between the vial and the magnet (Fig. 1). Four hardened, 25 mm in diameter, steel balls in the milling vial yielded the ball-to-powder weight ratio of 40:1 (Fig. 1). The samples were milled continuously for 1, 3, 10, 20, 50 and 100 h at ~225 RPM.

The crystalline structure of the as-milled powders was characterized with a Bruker D8 powder diffractometer using Cu Kα (not monochromated) radiation at the scan range from 10 to 90°, step size of 0.05°/s, accelerating voltage of 40 kV and a current of 30 mA. The nanograin (crystallite) size and lattice strain of phases residing in the milled powders were calculated from the broadening

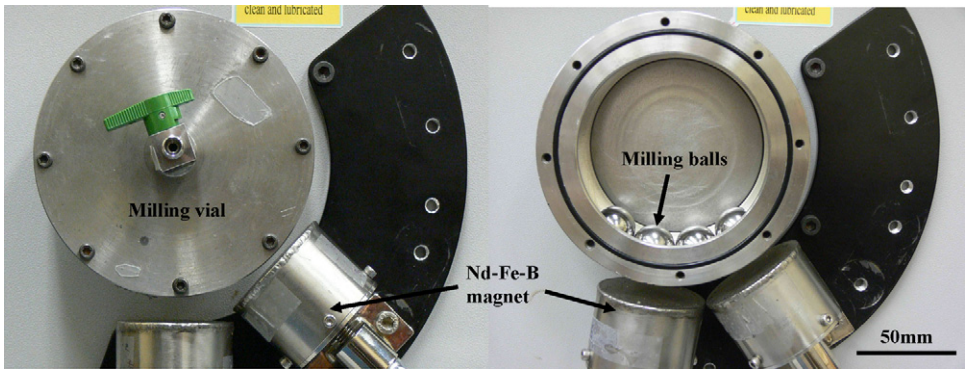

Fig. 1. Angular positions of Nd–Fe–B super-strong magnets at 6 and 8 o'clock for ball milling under high energy impact mode (IMP68) in the Uni-Ball Mill 5. The angular positions of external magnets can be changed at each of the controlled modes of milling [23–25].

of XRD peaks. Since the Bragg peak broadening in an XRD pattern is due to a combination of grain refinement (nanograin/crystallite) and lattice strains, it is customary to use computing techniques by means of which one can separate these two contributions. The separation of crystallite size and strain was obtained from Cauchy/Gaussian approximation by the linear regression plot according to the following equation [26]:

$$\frac{\delta^2(2\theta)}{\tan^2\theta} = \frac{K\lambda}{L}\left(\frac{\delta(2\theta)}{\tan\theta\sin\theta}\right) + 16e^2 \quad (3)$$

where the term $K\lambda/L$ is the slope, the parameter L is the mean dimension of the nanograin (crystallite) composing the powder particle, K is constant (~1) and e is the so-called "maximum" microstrain (calculated from the intercept), λ is the wave length and θ is the position of the analyzed peak maximum. The term $\delta(2\theta) = B[1 - (b^2/B^2)]$(rad) is the instrumental broadening-corrected "pure" XRD peak profile breadth [26] where B and b are the breadths in radians of the same Bragg peak from the XRD scans of the experimental and reference powder, respectively. They were calculated by the software Traces v. 6.5.1 as the full-widths at half maximum, FWHM, after $K\alpha_2$ stripping. A compound LaB_6, the National Institute of Standards and Technology (NIST) standard reference material (SRM) 660 was used as a reference for subtracting the instrumental broadening from FWHM. It must be noted that when the FWHM of the instrumental line profiles were obtained in this manner, the Bragg peaks for the LaB_6 SRM were at different 2θ angles than those of the analyzed phases in the milled powders. The interpolated FWHM values between angles for the SRM peaks were found using a calibration curve. Lattice parameters of the phases formed in the milled powders were determined using germanium as a standard with the software TRACES^{TM} v.6.5.1. Chemical composition of the particles in the milled powders was analyzed using a quantitative energy dispersive X-ray spectroscopy (EDS) (EDAX Pegasus 1200 EDS system).

The thermal behaviour of powders was studied by combined differential scanning calorimetry and thermogravimetric analysis (DSC-TGA) (TA INSTRUMENT Q600) of ~10 mg powder sample at a heating rate of 4 °C/min under a 100 ml/min nitrogen gas flow rate.

3. Results

3.1. Phase evolution as a function of milling time

The starting powder mixture was selected with the objective of initiating the following metathesis reaction

$$2NaBH_4 + MgCl_2 \rightarrow \text{ c-}Mg(BH_4)_2 + 2NaCl \quad (4)$$

where c-$Mg(BH_4)_2$ denotes a crystalline borohydride that would be expected.

Fig. 2 shows the XRD patterns of the powder mixture of $2NaBH_4$ and $MgCl_2$ after milling for 1, 3, 10, 20, 50 and 100 h. The powders after a short milling time consist of NaCl, $MgCl_2{\cdot}4H_2O$, retained $MgCl_2$ and $NaBH_4$-type phase (actually a $(Na,Mg)BH_4$ solid solution as will be discussed later). The presence of NaCl indicates that the reaction of Eq. (4) occurred during milling whereas the presence of retained $MgCl_2$, $MgCl_2{\cdot}4H_2O$ (most likely formed due to the exposure of retained $MgCl_2$ to moist air during XRD tests), and retained $NaBH_4$-type phase, show that the reaction of Eq. (4) has not been completed regardless of the milling duration even as long as 100 h. Fig. 3 shows the integrated intensity of the strongest (100%) (2 0 0) peak of $NaBH_4$-type phase ($(Na,Mg)BH_4$ solid solution) from Fig. 2 as a function of milling time. Apparently, it decreases with increasing milling time indicating that the volume fraction of $NaBH_4$-type phase decreases with milling time. In turn, this behavior confirms that the reaction of Eq. (4) between $2NaBH_4$ and $MgCl_2$ is gradually progressing during milling. Nakamori et al. [21,22] also reported that the synthesis is incomplete when $NaBH_4$ is used instead of $LiBH_4$ for certain compositions.

An important observation is that the peaks belonging to the retained $NaBH_4$-type phase in the milled powder mixtures are clearly shifted to the higher 2θ angles with respect to the peak positions of the reference as-received $NaBH_4$ (Fig. 2). The shifting may indicate a decrease of the lattice parameter and

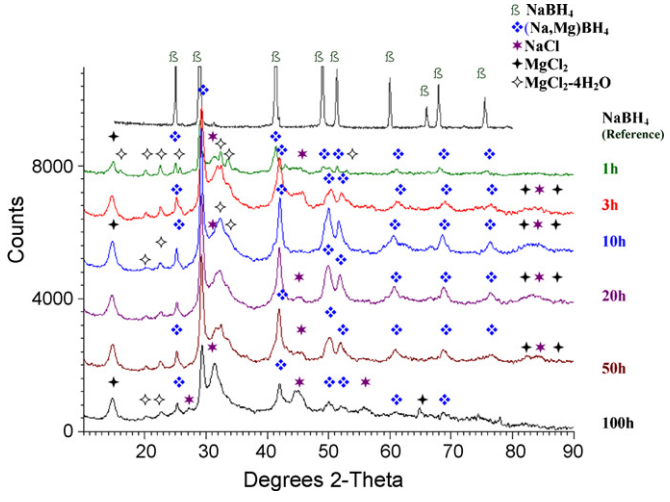

Fig. 2. XRD patterns of powder mixtures of $2NaBH_4$ and $MgCl_2$ after milling for 1, 3, 10, 20, 50 and 100 h under IMP68 mode.

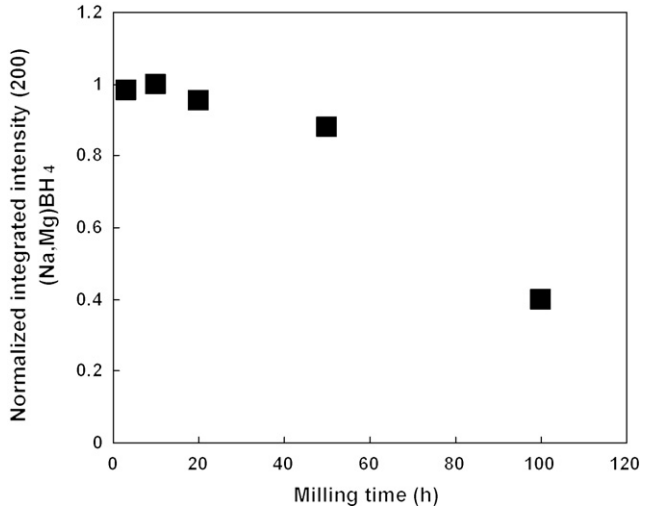

Fig. 3. Normalized integrated intensity of the strongest (100%) (2 0 0) peak of (Na,Mg)BH_4 solid solution phase vs. milling time.

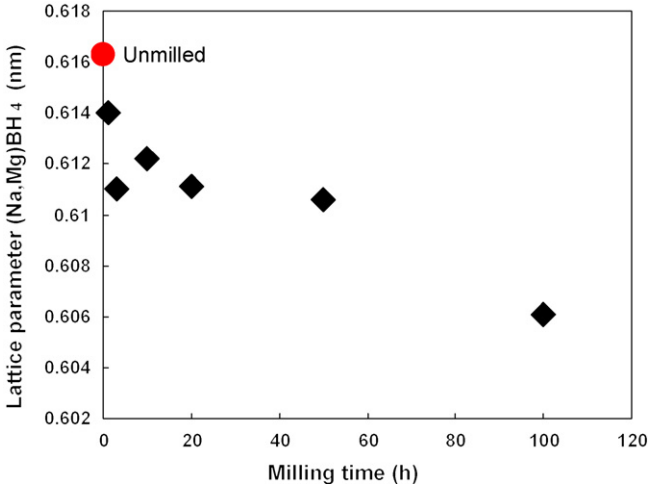

Fig. 4. Lattice parameter of (Na,Mg)BH_4 solid solution as a function of milling time.

shrinkage of the unit cell volume of $NaBH_4$. The lattice parameters and unit cell volume after various milling durations have been calculated and are listed in Table 1 . Fig. 4 shows a very clear trend such that the lattice parameter decreases monotonically with increasing milling time. Kumar and Cornelius [27] reported a shift of the peak positions to the higher 2θ angles and decrease of the lattice parameter and unit cell volume of a cubic α-$NaBH_4$ under increasing static pressure which subsequently led to pressure-induced structural transitions to a tetragonal β-$NaBH_4$ at 6.3 GPa of pressure and further to an orthorhombic phase at 8.9 GPa. Indeed, during ball milling, enormous pressure is applied to powder particles due to the impacts in a milling process which theoretically could result in the decrease of the lattice parameter. However, in the present work no structural transitions of a cubic $NaBH_4$-type phase are observed to occur with increasing milling time and the peak positions, although shifted, still correspond to an fcc-type crystalline lattice as can be seen in Fig. 2. $NaBH_4$-type phase retains its fcc-type cubic structure (ICCD PDF#38-1022 database v.1.30 1997) up to 100 h of milling duration.

Therefore, it is imperative to seek another explanation which can account for the shrinkage of the unit cell volume of $NaBH_4$. Since the retained $NaBH_4$-type phase has a reduced lattice parameter then apparently some Mg which has much smaller atomic radius of 0.1604 nm than that of Na which equals to 0.1858 nm [28], has dissolved in the original $NaBH_4$ lattice. In other words, as milling time increases, more and more Mg from the decomposing $MgCl_2$ diffuses into $NaBH_4$ lattice, substitutes Na in the lattice forming (Na,Mg)BH_4 solid solution and causes the shrinkage in the original unit cell volume of $NaBH_4$ (Table 1 and Fig. 4).

Table 2 shows that the (Na,Mg)BH_4 product after MCAS is nanocrystalline with the average grain size of ∼20 nm and a minimal lattice strain (<0.25%). The average grain size after a prolonged milling up to 100 h does not change a lot and is still in a nanometric range. This grain size range of (Na,Mg)BH_4 (∼19–22 nm) obtained under IMP68 mode is about three times smaller than the grain size of $NaBH_4$ after milling under low-energy shearing (LES) or impact (IMP2) modes as observed in our previous study [29]. It is clearly seen that under a very strong impact mode (IMP68) applied in the present work the rate of grain size decrease is faster than that under less energetic LES or IMP2 modes [29]. This might be due to the higher milling energy in IMP68 mode or the combination effect of higher milling energy and the presence of Mg in the $NaBH_4$ lattice. Since the nanostructure is formed after only 1 h of milling, the energy factor seems to have a stronger effect.

Table 1
Lattice parameters and unit cell volume of the $NaBH_4$-type phase in the milled powder mixtures of $2NaBH_4$ and $MgCl_2$

Milling time (h)	Lattice parameters (cubic) and unit cell volume			
	a (nm)		V ($\times 10^{-3}$) (nm^3)	
	Average	Error[a]	Average	Error[a]
Reference $NaBH_4$ (unmilled)	0.6163	0.0002	234.04	0.12
1	0.6140	0.0007	231.47	0.53
3	0.6110	0.0010	228.06	0.70
10	0.6122	0.0004	229.41	0.32
20	0.6111	0.0011	228.22	0.81
50	0.6106	0.0014	227.68	1.06
100	0.6061	0.0011	222.60	0.80

[a] Average lattice parameter, average volume and error are calculated by software TRACES^{TM} V.6.5.1 (error is *not* a standard deviation).

Table 2
Grain size D, strain e, numbers of the XRD peaks and linear regression R^2 of the (Na,Mg)BH_4 in the milled powder mixtures of $2NaBH_4$ and $MgCl_2$

Phase	Milling time (h)	Nanograin size (D) (nm)	Lattice strain (e)	R^2	No. of XRD peaks
$NaBH_4$	1	21	0	0.863	7
	3	17	2.5×10^{-3}	0.875	7
	10	22	2.5×10^{-3}	0.953	7
	20	19	3.5×10^{-3}	0.917	8
	50	18	1.8×10^{-3}	0.923	8
	100	19	7.9×10^{-4}	0.971	8

The most striking future of the XRD pattern in Fig. 2 is a complete absence of any peaks of crystalline $Mg(BH_4)_2$ despite the fact that NaCl has been formed as a product of the reaction of Eq. (4). Peaks in the XRD patterns of milled powders do not match those belonging to the crystalline ternary α- or β-$Mg(BH_4)_2$ hydride (ICCD PDF#26-1212 and 26–1213 database v.1.30 1997) which should be observed on the product side after completion of the reaction of Eq. (4). This is in contrast to the results of the exchange reaction ("metathesis reaction") of $NaBH_4$ with anhydrous magnesium chloride ($MgCl_2$) in diethyl ether [4,5] as reported by Russian researchers over 30 years ago who clearly synthesized a *fully crystalline* $Mg(BH_4)_2$ hydride. This is also in contrast to the successful MCAS reaction of $NaAlH_4$ and $MgCl_2$ in which we synthesized a nanocrystalline $Mg(AlH_4)_2$ in 5 h of milling time [30]. As mentioned earlier, Jeon and Cho [19] and Srinivasan et al. [20] reported the synthesis of *crystalline* $Zn(BH_4)_2$ by MCAS of $NaBH_4$ and $ZnCl_2$ for 0.5 h in a SPEX-8000 and for 0.5 to 8 h in a Fritsch P6 mill, respectively. After synthesis, clear XRD peaks were observed which after excluding NaCl peaks could be assigned to a crystalline $Zn(BH_4)_2$ phase in the milled powder. The presence of crystalline $Zn(BH_4)_2$ was also confirmed by the FT-IR spectra.

However, our results are in agreement with Nakamori et al. [21,22] who did not observe the XRD peaks of crystalline $M(BH_4)_n$ regardless of whether $LiBH_4$ or $NaBH_4$ was used. Only the Raman spectra confirmed the presence of "disordered" $M(BH_4)_n$ after MCAS.

3.2. Thermal behavior by DSC–TGA analysis

Thermal behavior of the milled $2NaBH_4$ and $MgCl_2$ powder was investigated by DSC and TGA. Fig. 5a–c show DSC–TGA curves of powder mixtures of $2NaBH_4$ and $MgCl_2$ after milling for 10–50 h upon heating to 420 °C while Fig. 5d shows DSC–TGA of powder after milling for 100 h upon heating to 500 °C. A strong endothermic peak is observed for all the powders at ∼298 °C. It must be noted that the heated samples transformed from a loose powder into a layer coated on the cru-

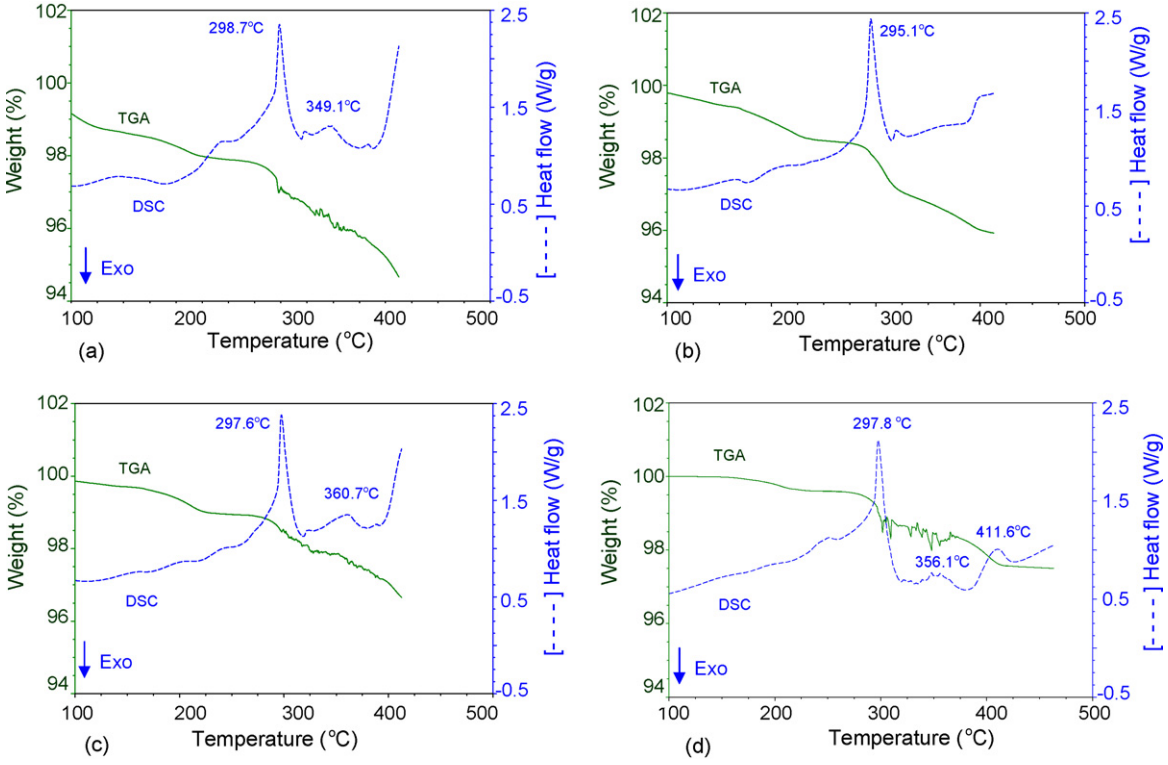

Fig. 5. DSC–TGA curves of powder mixtures of $2NaBH_4$ and $MgCl_2$ after milling for (a) 10 h, (b) 20 h, and (c) 50 h upon heating to 420 °C and (d) 100 h upon heating to 500 °C.

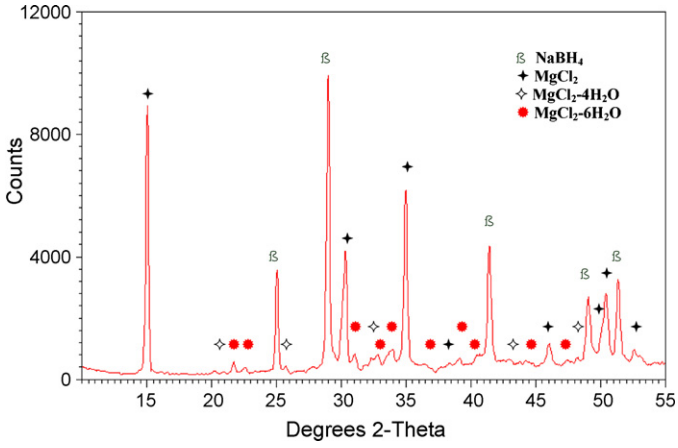

Fig. 6. XRD pattern of unmilled powder mixture of $2NaBH_4$ and $MgCl_2$ in a 2 to 1 stoichiometric ratio after annealing at 315 °C under 20 kPa of argon pressure for 0.5 h in a Sieverts-type apparatus.

cible wall after cooling down from ~298 °C in DSC–TGA tests. This is strong evidence of at least partial melting of the milled powder at ~298 °C. Unfortunately, due to a small amount of melted material that could be extracted from the crucible an XRD test was impossible to be carried out. Additionally, relatively strong endothermic peaks at ~349–360 and ~400–420 °C are also observed in the DSC curves.

Fig. 6 shows the XRD pattern of the *unmilled* powder mixture of $2NaBH_4$ and $MgCl_2$ after annealing under 20 kPa of argon at 315 °CC, which is slightly higher than the melting temperature (~298 °C) in Fig. 5a–d. The annealed powder mixture still contains $MgCl_2$ (partially hydrolyzed due to exposure to air during an XRD test) and $NaBH_4$. Apparently, annealing of the unmilled powder mixture at 315 °C does not result in the melting observed in the milled powder mixture which indicates that the DSC–TGA melting event at ~298 °C is strongly enhanced by pre-milling.

The TGA curves of milled powders and especially the one milled for 100 h show a three-stage weight loss at the temperature range of ~100–240, ~275–335 and ~335–420 °C (Fig. 5a–d). The approximate weight losses corresponding to each range of temperatures are listed in Table 3. The first small weight loss up to ~240 °C does not match to any thermal events

Table 3
Weight loss measured by TGA analysis for milled powder mixtures of $2NaBH_4$ and $MgCl_2$

Temperature range (°C)	Weight loss (wt.%)			
	10 h milled	20 h milled	50 h milled	100 h milled
100–240	1.3	1.3	0.9	0.4
275–335	1.4	1.5	1.0	1.2
335–420	1.8	1.0	1.2	0.9
Weight loss 275–420 °C	3.2	2.5	2.2	2.1
Total weight loss 100–420 °C	4.5	3.8	3.1	2.5

Note: Theoretical hydrogen capacity in a mixture of $2NaBH_4$ and $MgCl_2$ is ~4.7 wt.%.

in the corresponding DSC curves. However, magnesium chloride hydrate ($MgCl_2{\cdot}xH_2O$) starts to decompose at 95–115 °C [31]. As a result, the weight loss at ~100–240 °C is most likely due to the release of water which was absorbed by residual $MgCl_2$ during loading the powders into the DSC–TGA apparatus. The second TGA weight loss at ~275–335 °C (1.0–1.5 wt.% in Table 3) correlates well to the endothermic DSC peak at ~298 °C. As mentioned earlier, the morphology of the milled samples transforms from a loose powder into a layer welded on the crucible at ~298 °C in DSC–TGA test, which is evidence of melting. As a result, the second weight loss at the range ~275–335 °C can be attributed to the melting and a simultaneous decomposition of an unknown phase containing hydrogen, most likely "disordered" $Mg(BH_4)_2$ which gives an endothermic DSC peak with the maximum at ~298 °C. The third weight loss from ~335 to 420 °C (0.9–1.8 wt.% in Table 3) has a characteristic zig-zag shape of TGA curves in Fig. 5a, c, d and matches to the endothermic DSC peaks at ~349–360 and ~400–420 °C. It must also be pointed out that the weight loss in the 275–420 °C range decreases gradually with increasing milling time (Table 3).

4. Discussion

Based on the thermal behavior in DSC–TGA and the microstructural studies by XRD we can summarize the phase transformations occurring during milling and subsequent annealing in DSC in the following manner:

(1) Milling with MCAS.
- Partial reaction of $2NaBH_4 + MgCl_2 \rightarrow$ d-$Mg(BH_4)_2$ + 2NaCl (where "d-" is "disordered"); the presence of d-$Mg(BH_4)_2$ we invoke just on the basis of the results presented by Nakamori et al. [21,22] based on their Raman spectroscopy measurements (unfortunately, at the present moment we do not have an easy access to this technique).
- Formation of a solid solution (Na,Mg)BH_4 from the unreacted portion of $NaBH_4$ by Mg substitution into the lattice of $NaBH_4$ where the solutionizing effect increases with increasing milling time.

(2) $T \sim$ 100–240 °C; weight loss ~0.4–1.3 wt.%.
- Decomposition of magnesium chloride hydrate ($MgCl_2{\cdot}xH_2O$).

(3) $T \sim$ 275–335 °C; weight loss ~1.0–1.5 wt.%.
- Melting and a simultaneous full or partial decomposition of d-$Mg(BH_4)_2$ into β-MgH_2, B and H_2 which gives an endothermic DSC peak with the maximum at ~298 °C.

(4) $T \sim$ 335–420°C; weight loss ~1.0–1.8 wt.%.
- A small DSC heat flow peak at ~350–360 °C in Fig. 5a, c, d remains unexplained.
- Decomposition of β-MgH_2, with the peak maximum around 410–420 °C.
- A "zig-zag" shape of TGA curve in Fig. 5a, c, d suggests some volatility of the decomposition reaction in this range, in particular, for the sample milled for 100 h (Fig. 5d); the cause of this volatility is unclear but might be related to the further decomposition of the remnants of d-$Mg(BH_4)_2$.

The thermal behavior in the 275–335 °C range described above is similar to the thermal events reported by Stasinevich and Egorenko [4] and Konoplev and Bakulina [5]. These authors reported that the thermal effect which they observed at 304–323 °C was due to the melting with simultaneous decomposition of crystalline β-$Mg(BH_4)_2$ and the formation of magnesium hydride, boron and hydrogen. The DSC thermal endothermic effect with the peak at ∼298 °C, observed in (Fig. 5a–d), is close to the temperature range reported by the Russian authors. The presence of d-$Mg(BH_4)_2$ in the milled mixture is also supported strongly by Fig. 6 which shows that the unmilled mixture does not melt most likely due to the absence of d-$Mg(BH_4)_2$ which has a melting range around 300 °C.

Stasinevich and Egorenko [4] and Konoplev and Bakulina [5] also observed a peak at the 402–420 °C range which they assigned to the decomposition of magnesium hydride which agrees with the heat flow peak around 410–425 °C in Fig. 5a–d which we also assign to the decomposition of β-MgH_2.

Despite a general agreement with the early works on the synthesis and thermal decomposition of crystalline β-$Mg(BH_4)_2$, one outstanding issue remains unclear. Why did the "wet" exchange reaction between $NaBH_4$ and MgC_2 in diethyl ether as carried out by the Russian researchers over 30 years ago [4,5] result in a perfectly crystalline $Mg(BH_4)_2$ whereas MCAS gives a "disordered" $Mg(BH_4)_2$? Is it possible that a "disordered" $Mg(BH_4)_2$ forms only if ball milling is applied to its synthesis? To answer these important questions more research is still required. At this point it should be pointed out that the formation of (Na,Mg)BH_4 solid solution might have prevented the synthesis of a large amount of crystalline $Mg(BH_4)_2$ hydride. Solid solution plays a detrimental role in the synthesis of a complex hydride in the Mg–Al–H system. Recently, we have reported that once a solid solution Al(Mg) is formed, a complex hydride $Mg(AlH_4)_2$ cannot be synthesized by a direct mechano-chemical synthesis (MCS) process using a reactive mechanical alloying of elemental powders and Mg–Al alloys [31]. For the present work, it is hypothesized that the presence of (Na,Mg)BH_4 solid solution in the MCAS process of $NaBH_4$ and $MgCl_2$ might have inhibited the reaction of Eq. (4). Once solid solution is formed, the amount of Mg is not sufficient to form a large amount of crystalline $Mg(BH_4)_2$ hydride. Instead, a "disordered" $Mg(BH_4)_2$ is possibly formed.

Finally, it is to be noted that if one compares enthalpy of formation of $NaBH_4$ and $NaAlH_4$, it can be found that enthalpy of formation of $NaBH_4$ (−191.84 kJ/mol) is larger than that of $NaAlH_4$ (−15.5 kJ/mol) [32]. As a result, MCAS of $NaBH_4$ and NaCl might be more difficult than that of $NaAlH_4$ and NaCl as we reported in [30].

5. Conclusions

A unique discovery made in this work is the formation of (Na,Mg)BH_4 solid solution in the powder mixture of $2NaBH_4$ and $MgCl_2$ processed by mechano-chemical activation synthesis (MCAS) using ball milling in a magneto-mill. The solutionizing effect becomes more intense as milling time increases. Although the result of XRD analysis in the present work does not indicate the presence of a crystalline $Mg(BH_4)_2$ hydride, the similarity of thermal events in the DSC curve in the milled powder mixtures to those of $Mg(BH_4)_2$ reported by Stasinevich and Egorenko [4], Konoplev and Bakulina [5] and Nakamori et al. [21,22] might indicate the possibility of presence of a small amount of a "disordered" $Mg(BH_4)_2$ in the in the milled powder mixture, as specifically reported by Nakamori et al. [21,22]. It is hypothesized that the presence of (Na,Mg)BH_4 solid solution in the MCAS process inhibits the formation of crystalline $Mg(BH_4)_2$. Once a solid solution is formed, the amount of Mg is insufficient to form a large amount of perfectly crystalline $Mg(BH_4)_2$ hydride and more "disordered" $Mg(BH_4)_2$ (d-$Mg(BH_4)_2$) hydride forms. However, the nature of atomic bonds in the milled powder mixture is needed to be analyzed (e.g. by Raman spectra) to confirm the presence of a "disordered" $Mg(BH_4)_2$ phase. Regardless of the nature of the synthesized hydride phase the milled powders desorb hydrogen within the 275–420 °C temperature range and the total amount desorbed is the largest for the powder milled for 10 h (∼3.2 wt.%) and gradually decreases with increasing milling time reaching ∼2.1 wt.% for the powder milled for 100 h. However, regardless of the milling time the total amount of hydrogen desorbed within 275–420 °C is always less than the theoretical hydrogen capacity in a mixture of $2NaBH_4$ and $MgCl_2$ which was used for the synthesis.

Acknowledgements

This work was financially supported by a grant from the Natural Sciences and Engineering Research Council of Canada which is gratefully acknowledged.

References

[1] J.A. Ritter, A.D. Ebner, J. Wang, R. Zidan, Mater. Today 6 (9) (2003) 18–23.
[2] A. Züttel, P. Wenger, S. Rentsch, P. Sudan, Ph. Mauron, Ch. Emmenegger, J. Power Sources 118 (2003) 1–7.
[3] L. Schlapbach, A. Züttel, Nature 414 (2001) 353–358.
[4] D.S. Stasinevich, G.A. Egorenko, Russian J. Inorg. Chem. 13 (1968) 341–343.
[5] V.N. Konoplev, V.M. Bakulina, Izv. Akad. Nauk SSSR 1 (1971) 159–161.
[6] M. Fichtner, Adv. Eng. Mater. 7 (2005) 443–455.
[7] R.A. Varin, T. Czujko, Mater. Manuf. Proc. 17 (2002) 129–156.
[8] J. Huot, G. Liang, R. Schulz, Appl. Phys. A 72 (2001) 187–195.
[9] A. Zaluska, L. Zaluski, J.O. Ström-Olsen, Appl. Phys. A 72 (2001) 157–165.
[10] A. Zaluska, L. Zaluski, J.O. Ström-Olsen, J. Alloys Compd. 288 (1999) 217–225.
[11] R.A. Varin, Ch. Chiu, Z. Wronski, A. Calka, Solid State Phenomena 128 (2007) 47–52.
[12] Z. Wronski, R.A. Varin, C. Chiu, T. Czujko, A. Calka, J. Alloys Compd. 434/435 (2007) 743–746.
[13] D. Goerrig, German Patent DE1077644 (1958).
[14] T.N. Dymova, V.N. Konoplev, A.S. Sizareva, D.P. Aleksandrov, Russ. J. Coord. Chem. 25 (5) (1999) 312–315.
[15] T.N. Dymova, N.N. Mal'tseva, V.N. Konoplev, A.I. Golovanova, D.P. Aleksandrov, A.S. Sizareva, Russ. J. Coord. Chem. 29 (6) (2003) 385–389.
[16] M. Mamatha, B. Bogdanović, M. Felderhoff, A. Pommerin, W. Schmidt, F. Schüth, C. Weidenthaler, J. Alloys Compd. 407 (2006) 78–86.

[17] M. Mamatha, C. Weidenthaler, A. Pommerin, M. Felderhoff, F. Schüth, J. Alloys Compd. 416 (2006) 303–314.
[18] Y. Kim, E.-K. Lee, J.-H. Shim, Y.W. Cho, K.B. Yoon, J. Alloys Compd. 422 (2006) 283–287.
[19] E. Jeon, Y.W. Cho, J. Alloys Compd. 422 (2006) 273–275.
[20] S. Srinivasan, E. Lee Stefanakos, Y. Goswami, Proceedings WHEC 13-16 June 2006, Lyon, France, 2006, pp. 1/6–6/6.
[21] Y. Nakamori, K. Miwa, A. Ninomiya, H. Li, N. Ohba, S.-I. Towata, A. Züttel, S.-I. Orimo, Phys. Rev. B74 (2006) 045126.
[22] Y. Nakamori, H.-W. Li, K. Kikuchi, M. Aoki, K. Miwa, S. Towata, S. Orimo, J. Alloys Compd. 446–447 (2007) 296–300.
[23] A.P. Calka, Radlinski, Mater. Sci. Eng. A 134 (1991) 1350–1353.
[24] Patents: WO9104810, US5383615, CA2066740, EP0494899, AU643949.
[25] R.A.V. Calka, in: T.S. Srivatsan, R.A. Varin, M. Khor (Eds.), Proceeding of the International Symposium on Processing and Fabrication of Advanced Materials IX PFAM-IX, ASM International, Materials Park, OH, 2001, pp. 263–287.
[26] H.P. Klug, L. Alexander, X-ray Diffraction Procedures for Polycrystalline and Amorphous Materials, John Wiley & Sons, New York, 1974, pp. 618–708.
[27] R.S. Kumar, A.L. Cornelius, Appl. Phys. Lett. 87 (2005) 261916.
[28] D.R. Askeland, P.P. Phulé, The Science and Engineering of Materials, fourth ed., Brooks/Cole-Thomson Learning Inc., Pacific Grove, 2003, pp. 980–981.
[29] R.A. Varin, Ch. Chiu, J. Alloys Compd. 397 (2005) 276–281.
[30] R.A. Varin, Ch. Chiu, T. Czujko, Z. Wronski, J. Alloys Compd. 439 (2007) 302–311.
[31] R.A. Varin, T. Czujko, Z. Wronski, Nanotechnology 17 (2006) 3856–3865.
[32] CRC Handbook of Chemistry and Physics, 85th ed. http://www.hbcpnetbase.com.